Combining light sheet microscopy and expansion microscopy for fast 3D imaging of virus-infected cells with super-resolution

Luca Mascheroni[1]*, Katharina M. Scherer[1]*, Edward Ward[1], Oliver Dibben[2] and Clemens F. Kaminski[1]

[1] Department of Chemical Engineering and Biotechnology, University of Cambridge, Cambridge, UK
[2] Flu-BDP, AstraZeneca, Liverpool, UK

E-mail: cfk23@cam.ac.uk

* These authors contributed equally.

Abstract

Expansion microscopy is a sample preparation technique that enables the optical imaging of biological specimens at super-resolution, owing to their physical magnification. Expansion is achieved by embedding the sample in a polymer matrix that swells upon water absorption. The technique makes use of readily available chemicals and does not require sophisticated or custom-made equipment, and therefore offers super-resolution to laboratories that are not specialised in microscopy technologies. The expanded samples are hydrogels that can be imaged with any microscope, as long as the gelled sample can be mounted on that system setup. Here, we focus on the expansion and optical imaging of live attenuated influenza vaccine (LAIV)-infected human cells. We present a protocol to image expanded samples on a light sheet microscope and generate high contrast 3D reconstructions of whole infected cells. The results are superior to those achievable with either widefield or confocal imaging methods for expanded samples and allowed us to visualise structural features of compartments in the infected cells occupied by viral proteins that were not visible before the expansion. In order to promote the optimal combination of expansion and light sheet microscopy, we include a detailed video protocol for the mounting and imaging of gelled samples using a light sheet microscope. The protocol is applicable for super-resolution imaging of virus-host cell interaction in general and we expect that the methodology can greatly contribute to further the research in the field of virology.

Keywords: super-resolution, expansion microscopy, light sheet microscopy, 3D imaging, virus imaging.

1. Introduction

Expansion microscopy is a technique that relies on the physical magnification of biological samples in order to visualise details that are spaced more closely than the diffraction limit of light (~300 nm).[1,2] The physical expansion is achieved by embedding fixed specimens in a polymer matrix that can absorb water, forming a so-called hydrogel. This approach generates volumetrically isotropic expansion and allows the bypassing of the diffraction barrier of light microscopy without any need for sophisticated instruments, enabling laboratories that possess standard fluorescence microscopes to image their samples at super-resolution. Despite the great potential of expansion microscopy, the nature of the

expanded sample places some limitations on its use. Firstly, the hydrogels are challenging to image using conventional microscopes: such samples are bulky and mechanically unstable, making mounting and long-term imaging more challenging compared to conventional samples (for example, cells adherent on a glass slide). Secondly, when the hydrogel is placed in a dish and imaged through the bottom, the 'vertical' expansion of the sample hinders the imaging of the whole volume of the specimen using high numerical aperture (NA) objectives, which usually have short working distances. Moreover, the use of oil-immersion objectives generates a refractive index mismatch with the water-based hydrogels, which causes optical aberrations. Finally, the expansion process dilutes the fluorophore concentration, decreasing the fluorescence intensity up to a hundredfold, which hinders the imaging of expanded samples using microscopes incapable of collecting a large number of photons or those requiring very high fluorescent signals.

Expanded samples have so far been imaged mainly using confocal microscopes.[2] However, a confocal microscope might not be optimal for the imaging of expanded samples: the weak fluorescence intensity of the expanded specimens is best recorded with a setup that is more photon-efficient than a confocal microscope. Light sheet microscopy is such a technique. Nonetheless, reports on the combination of light sheet microscopy with sample expansion have been limited so far.[6–8]

In light sheet microscopy, the optical pathways of excitation and detection are geometrically decoupled such that the sample is illuminated with a thin sheet of laser light, and detection is performed along an axis orthogonal to the illumination. This separation of excitation and detection light paths maximises detection efficiency by minimising out-of-focus fluorescence. The axial confinement of the excitation results furthermore in dramatically reduced photobleaching. For detection, fast cameras with high quantum efficiency can be used, and thus imaging speed can be increased by orders of magnitude compared to point-scanning techniques.

The principle of light sheet microscopy was developed more than a century ago by Siedentopf and Zsigmondy as ultramicroscopy.[3] It was rediscovered by developmental biologists at the beginning of the 21st century[4] and its popularity has increased ever since. The high spatiotemporal resolution was impressively demonstrated for high-speed imaging of embryonal development,[5] neural activity,[6] cardiac dynamics,[7,8] and physiologically representative subcellular imaging.[9] Despite all the advantages, a complication which regularly arises in light sheet microscopy concerns the mounting of the samples which has to be compatible with the two-objective configuration of the method and solutions often need to be customised for the specific experimental configuration in use. Nowadays, commercial setups are available, and a lot of effort is still invested in the technical development of designs that are simpler to use and that improve the versatility and utility of the method.

In this work, we study the suitability of expansion microscopy and light sheet microscopy for the imaging of virus-infected samples using human A549 cells infected with live attenuated influenza vaccine (LAIV), a modified low-virulence variant of the influenza A virus that is the basis of flu vaccine formulations and sold under the names Fluenz (USA and Canada) and FluMist (Europe).[10,11] We show that expansion microscopy is particularly well suited to study host-cell vaccine interactions helping to understand underlying biomolecular mechanisms of the vaccine. Optical imaging at super-resolution is required in order to dissect the interplay of viral proteins and substructures with cell organelles, which often have dimension comparable to, or smaller than, the diffraction limit of light (~300 nm). However, imaging entire infected cells in multiple colours to build a full 3D picture of the infected cell is challenging using alternative super-resolution techniques, like dSTORM[10] and STED,[11] due to their long acquisition times and proneness to photobleaching.

Here, we first describe the expansion of infected cells using a published expansion microscopy protocol. We then explain the imaging of the infected expanded cells on a light sheet microscope, and for comparison, also on widefield and confocal microscopes. By combining expansion microscopy with light sheet microscopy, we demonstrate how high-contrast 3D models of whole LAIV-infected cells can be easily reconstructed at super-resolution in four colour channels, highlighting new features of three-dimensional structures carrying viral proteins that were not distinguishable before the sample expansion. Finally, we present a detailed video protocol on the mounting and imaging of expanded

samples using a light sheet microscope. The aim is to make this technique available to the wider community and so that the power of light sheet and expansion microscopy can be harnessed for addressing a series of biological problems that require super-resolution and volumetric sectioning in multiple colours.

2. Materials and methods

2.1 Chemicals

Methanol-free formaldehyde was purchased from Thermo Fisher Scientific; the ampoules were used immediately after opening and any leftover formaldehyde discarded. All chemicals used for sample expansion (glutaraldehyde 50% in water, sodium acrylate, N, N'-methylenbisacrylamide, acrylamide, Proteinase K) were purchased from Sigma Aldrich and used as received.

2.2 Antibodies

Mouse anti-influenza A nucleoprotein (ab20343) and rabbit anti-beta tubulin (ab6046) primary antibodies were purchased from Abcam. Detection was achieved using polyclonal goat secondary antibodies: an ATTO647N-conjugated anti-mouse antibody was purchased from Sigma Aldrich, while an AlexaFluor488 (AF488)-conjugated anti-rabbit antibody was purchased from Invitrogen.

2.3 Virus

The Live Attenuated Influenza Virus (LAIV, 9.2 TCID50/mL) derived from the wildtype Influenza A strain A/New Caledonia/20/99 was provided by AstraZeneca (Speke, Liverpool).

2.4 Cell cultures

A549 cells were purchased from the European Collection of Authenticated Cell Cultures (ECACC). The cell line was cultured at 37°C and 5% CO_2 in Dulbecco-modified MEM (Sigma Aldrich) supplemented with 10% heat-inactivated foetal bovine serum (Gibco), antibiotics/antimycotics (100 units/mL penicillin, 100 µg/mL streptomycin, 0.025 µg/mL Gibco Amphotericin B, Gibco) and 2 mM L-glutamine (GlutaMAX, Gibco). Cultures at ~80% confluency were routinely split into T-75 polystyrene flasks.

2.5 Infection of A549 cells with LAIV

A549 cells were plated onto 13 mm round coverslips in 4-well plates at 60,000 cells per well, 16 hours before infection. The next day, cells were infected with LAIV at 10 PFU per cell. After one hour of incubation at 37°C and 5% CO_2, the medium was exchanged with fresh new medium. Cells were fixed 9 hours post infection (hpi), permeabilised and labelled with antibodies according to procedures described below.

2.6 Immunostaining

Infected cells were fixed by incubation with 4% methanol-free formaldehyde and 0.1% glutaraldehyde in PBS for 15 minutes at room temperature, washed three times with PBS and then permeabilized by incubation with a 0.25% solution of Triton X-100 in PBS for 10 minutes. Unspecific binding was blocked by incubating with 10% goat serum in PBS for 30 minutes at room temperature. Without washing, the samples were incubated with the primary antibody, diluted 1:200 in PBS containing 2% BSA (bovine serum albumin) for 1 hour at room temperature, or overnight at 4°C. After three washes in PBS, the samples were incubated with the secondary antibody, diluted 1:400 in PBS containing 2% BSA, for an hour at room temperature in the dark. Samples were then washed 3 times with PBS. Samples that were not meant for expansion microscopy were counterstained with DAPI

nuclear dye (10 µg/mL in PBS for 10 minutes at room temperature). Finally, the coverslips were mounted on glass slides using a Mowiol-based mounting medium. Alternatively, samples were expanded as detailed below.

2.7 Expansion and imaging of samples

The expansion of samples was achieved following a published protocol.[12] Nuclear staining was performed after the first round of expansion, using DAPI, 10 µg/mL in water for 20 minutes. In order to image the expanded gels on the widefield and confocal microscopes, they were cut using a glass coverslip as a knife to fit in glass-bottom Petri dishes, which were pre-coated with poly-L-lysine (0.02% in water for 30 minutes). Alternatively, the gels were imaged with the light sheet microscope, by cutting a strip of gel with cells facing up, which was then glued on a 24x50 mm glass coverslips using cyanoacrylate-based super-glue (Henkel). The slide was left to cure for two minutes and then placed in an imaging chamber and filled with milli-Q water. This process is documented in detail in Supporting Video 1.

2.8 Microscopes

The light sheet microscope was home built using the inverted selective plane illumination microscopy (iSPIM)[13] design for which parts were purchased from Applied Scientific Instrumentation (ASI, Eugene, USA) including controller (TG8_BASIC), scanner unit (MM-SCAN_1.2), right-angle objective mounting (SPIM-K2), stage (MS-2K-SPIM) with motorized Z support (100 mm travel range, Dual-LS-100-FTP) and a filter wheel (FW-1000-8). All components were controlled by Micro-Manager, using the diSPIM plugin from ASI. The setup was equipped with a 0.3 NA excitation objective (Nikon 10x, 3.5 mm working distance) and a 0.9 NA detection objective (Zeiss, W Plan-Apochromat 63x, 2.1 mm working distance) to increase spatial resolution and fluorescence signal collection. Lasers were fibre-coupled into the scanner unit. An sCMOS camera (ORCA-Flash 4.0, Hamamatsu, Hamamatsu-City, Japan) was used to capture fluorescence. DAPI was excited with 445 nm (OBIS445-75 LX), AlexaFluor488 with 488 nm (OBIS488-150 LS) and ATTO647N with 647 nm (OBIS647-120 LX). For fluorescence detection, respective emission filters were used (DAPI: BrightLineFF01-474/27, AF488: BrightLineFF01-540/50, ATTO647N: BrightLineFF0-680/42). Filters were purchased from Semrock (New York, USA).

The widefield microscope was home built and parts were purchased from the following suppliers: frame (IX83, Olympus, Tokyo, Japan), stage (Prior, Fulbourn, UK), Z drift compensator (IX3-ZDC2, Olympus, Tokyo, Japan), plasma light source (HPLS343, Thorlabs, Newton, USA), and camera (Clara interline CCD camera, Andor, Belfast, UK) of the custom-built wide-field microscope were controlled by Micro-Manager. Respective filter cubes for DAPI (excitation 350 nm, dichroic mirror 353 nm, emission 460 nm), AF488 (excitation 500 nm, dichroic mirror 515 nm, emission 535 nm) and ATTO647N (excitation 560 nm, dichroic mirror 585 nm, emission 630 nm) were used for selecting excitation and detecting fluorescence. The images were acquired with an Olympus PlanApoU 60x/1.42 oil objective lens.

The confocal microscope was a commercial Leica TCS SP5. The following excitation lasers were used: 405 nm (DAPI), 488 nm (AF488), 647 nm (ATTO647N). The following detectors were used: DAPI 420-450 nm; AlexaFluor488 500-600 nm; ATTO647N 660-800 nm. The images were acquired with a 63x/1.42 oil objective lens.

2.9 Data analysis

Vesicle size in expanded samples that were imaged using light sheet microscopy was analysed using ImageJ. Data were plotted in GraphPad Prism (GraphPad Software, US).

3. Results and discussion

3.1 Infection, staining and expansion of cells

A549 cells, from human alveolar carcinoma, are a common model for the study of LAIV infection and replication.[11] We incubated the cells with the LAIV particles at 10 PFU for one hour, then we exchanged the medium and let the internalised viral particles progress in their infection cycle before fixation. The LAIV virions are not fluorescent, therefore, immunostaining of the viral proteins is necessary in order to study the infection progression using optical fluorescence microscopy. Here, we stained the LAIV nucleoprotein (NP), a structural protein that packs the viral RNA inside of the virus.[14] Additionally, we stained the cell microtubules and the cell nuclei, in order to study the interaction between the viral particles and the cell organelles. A picture of the stained infected cells before expansion, imaged on a confocal microscope, is shown in Figure 1. The resolution of the non-expanded images is enough to localise the viral nucleoprotein (NP) in the cell cytosol. However, the image resolution is too low to clarify the exact NP localization, form, and interaction with other cell structures.

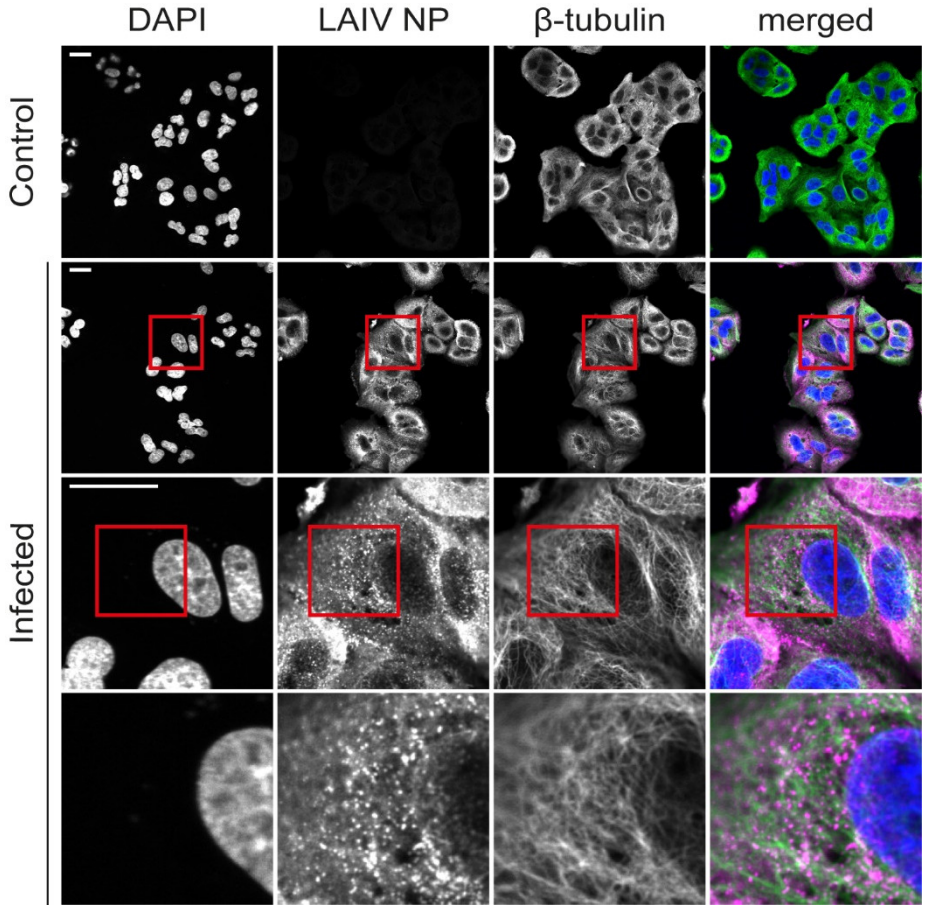

Figure 1: Non-expanded A549 cells were infected with live attenuated influenza virus (LAIV). Cells were fixed 9 hours post infection and images recorded at a confocal microscope. Immunostaining was used to fluorescently label LAIV nucleoprotein (NP, magenta) and microtubules (green) whereas DAPI staining was used for labelling of the nuclei (blue). Scale bar 25 µm. Size of images in bottom row 25 x 25 µm^2.

After immunostaining, the cells were expanded using a published expansion microscopy protocol.[12] Briefly, expansion microscopy works by synthesising a polymer matrix *in situ*, which cross-links the protein structures of the sample. The sample, now embedded within the gel, is then enzymatically digested by proteases in order to cleave the cells rigid structures such as the cytoskeleton. Without digestion, the gelled sample would not expand; however, the linking to the gel matrix guarantees that the cleaved proteins are not lost and that they keep their relative positions. Finally, the gel is placed in deionised water to expand. The expansion process spatially separates the fluorophores that are spaced more closely than the microscope resolution, increasing the level of detail in the final image. A

schematic representation of the steps of the expansion microscopy protocol is shown in Supporting Figure 1.

3.2 Mounting expanded samples for microscopy

The expanded gels are unconventional imaging samples: since they mainly consist of water, they are very fragile and unsteady. In order to image the gelled samples on inverted confocal or widefield microscopes, we cut them to fit into glass-bottom Petri dishes with cells facing down (Figure 2A, left). One issue we encountered while imaging the gels in this configuration is their wobbling and drifting during the image acquisition. To minimise this issue, we pre-coated the glass bottoms of the dishes with poly-L-lysine, which improves gel adherence. However, this is not always enough to keep the gels sufficiently still, especially during long-term imaging. The use of cyanoacrylate-based glue to keep the gels in place has been suggested,[15] although gluing the gels in this configuration requires the glue to be placed directly in contact with the cell-containing side of the sample, possibly deteriorating the embedded biological structures. Moreover, the use of glue makes the glass-bottom dishes non-reusable.

In order to image the expanded samples using a light sheet microscope, a small gel strip was cut and attached to a glass slide (24x50 mm) using super-glue, with cells facing up (Figure 2A, right). In this configuration, the glue was not in direct contact with the cells and this prevented problems associated with gel wobbling or drifting. Cutting the gel into a strip makes it able to fit in between the two light sheet objectives; this configuration enables the imaging of the whole depth of the sample. Moreover, the light sheet microscope is equipped with water-dipping objectives, which eliminates any possible optical aberration due to refractive index mismatches with the (water-based) gels. On the contrary, the high NA objectives used on the widefield and confocal microscopes had short working distances, preventing visualisation of the deepest planes of the gel. A step-by-step procedure for the mounting of expanded samples on a light sheet microscope is depicted in Figure 2B. A detailed video protocol of this procedure is demonstrated in Supporting Video 1, where we show how we cut the gelled sample and glued it to the glass slide of the imaging chamber of the light sheet microscope.

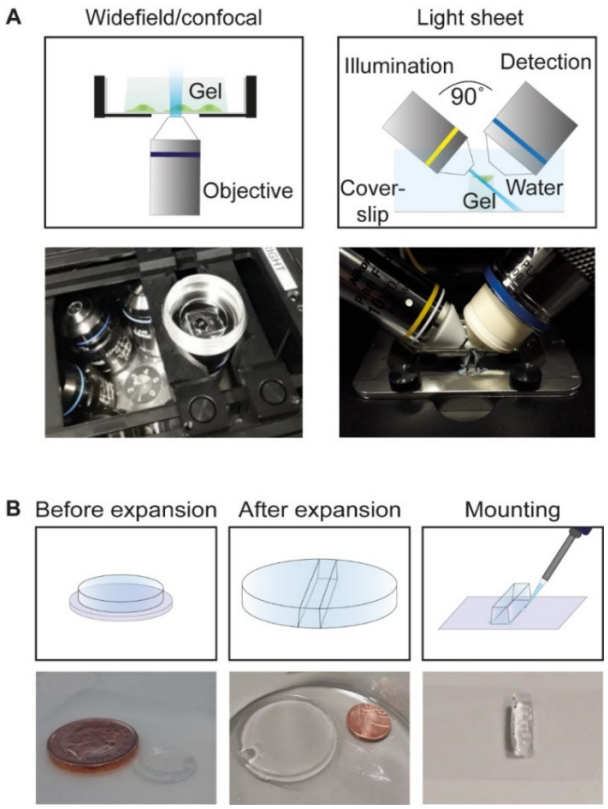

Figure 2: (A) Schematic representation of gel mounting for widefield/confocal microscopy (left) on an inverted microscope and for light sheet microscopy on a custom-built iSPIM setup (right). (B) Step-by-step procedure for light sheet microscopy.

3.3 Comparison of imaging modalities

We compared light sheet microscopy of expanded samples with two commonly used conventional fluorescence microscopy techniques, widefield and confocal laser scanning microscopy (CLSM). The working principles of all three techniques are illustrated in Figure 3A. When imaging a sample using a widefield microscope, the whole fluorescent specimen is excited which results in considerable out-of-focus light derived from fluorophores that lie outside of the focal plane, producing high background signals and low image contrast. A confocal laser scanning microscope mitigates this problem by using a point-source for illumination and pinholes to filter out out-of-focus fluorescence. As a result, CLSM features better image contrast compared to widefield microscopy. However, the requirement for scanning the point sequentially across the sample decreases the acquisition speed significantly and reduces the number of signal photons that can be collected. A light sheet microscope combines the advantages of a confocal laser scanning and a widefield microscope: here the sample is illuminated with a thin sheet of light that excites only those fluorophores that lie in the focal plane of the sample. Thus, the signal is only generated from the illuminated fluorophores and those in out-of-focus planes are not excited and therefore do not contribute to image blur. Speed is not reduced due to widefield detection with a camera.

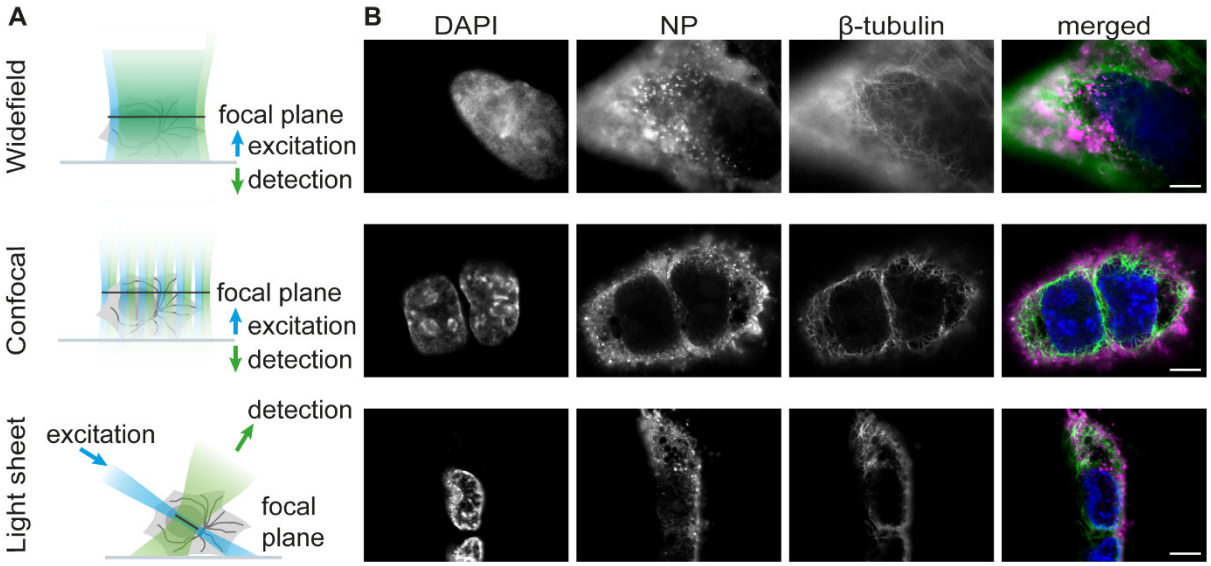

Figure 3: (A) Comparison of three different fluorescence microscopy techniques for imaging of expanded samples. (B) Expanded A549 cells infected with live attenuated influenza vaccine (LAIV). Cells were fixed 9 hours post infection, immunostained, expanded and imaged using widefield, confocal or light sheet microscopy. Merged images show LAIV nucleoprotein in magenta, microtubules in green and cell nuclei in blue. Scale bar 25 µm.

Using all three microscopy techniques, we imaged A549 cells that were infected with live attenuated influenza virus (LAIV), fixed 9 hours post-infection, immunostained and expanded as described in Section 3.1. Exemplary images showing the cell nucleus, the viral nucleoprotein (NP) and microtubules are displayed in Figure 4B. As expected, we observed the lowest amount of bleaching by using the light sheet microscope. During the acquisition of an image stack consisting of 100 frames spaced by 500 nm, photobleaching of the sample after the acquisition of one stack was minimal. On the widefield microscope, photobleaching of the sample during the acquisition of one image stack was also low. CLSM resulted in substantial photobleaching of the sample. Due to scanning, the speed of CLSM was significantly reduced compared to widefield and light sheet microscopy. Whereas the acquisition for one frame in four colours was in the range of ten minutes, it took only a few seconds on the widefield and light sheet microscopes. This long acquisition time, combined with the high (>80 mW) laser power used to boost the fluorescent signal, makes the confocal microscope unsuitable for recording z-stacks, since the photobleaching of the gel portion was almost complete after acquiring only one frame.

It must be noted that, when acquiring confocal images, the microscope pinhole was set to a value of 2.0 Airy units (in contrast to the pre-set value 1.0 Airy units), which made it possible to boost the signal of the weakly fluorescent sample, at the cost of reduced out-of-focus light filtering. In the imaging of brighter samples on a confocal setup, reducing the pinhole size may increase background rejection and achieve contrast levels comparable to (or higher than) light sheet microscopy. The reduced sensitivity of the confocal system reflects the fundamental difference in the detection of the fluorescent signal. In the confocal setup the photomultiplier used to measure the fluorescence has approximately half the quantum efficiency than that of the sCMOS camera used for light sheet imaging (~40% compared to ~80% at the wavelengths used). This doubles the number of photons measured in the light sheet system, greatly increasing the signal to noise ratio (SNR). It follows that, whilst the confocal and light sheet images are comparable in terms of contrast, light sheet microscopy outperforms confocal microscopy in terms of noise performance.

To quantify the increase in SNR, we measured the amount of high-frequency noise present in the images. Given the low number of photons collected when imaging expanded samples, Poisson noise dominates in the final images. As this noise is added on a pixel-by-pixel basis, it appears as sub-diffraction speckle, which means that the noise can be quantified by measuring the amount of sub-diffraction information in the images. We performed this by convolving the acquired image with the theoretical point spread function (PSF) of the instrument and calculating the root mean squared error (RMSE) between the resulting image and the original acquired image. Convolving the acquired image with the PSF of the system suppresses sub-diffraction features (such as Poisson noise) while leaving the true sample structure unaffected. We calculated this RMSE value (E) for visually similar patches of the LAIV nucleoprotein channel spanning the same field of view (Supporting Figure 2). Of the techniques tested, widefield microscopy performs the best in terms of high-frequency noise, producing the lowest error (E = 0.0166). This is likely because the low-frequency out-of-focus signal – rather than high-frequency Poisson noise- is the dominant factor in reducing contrast. Of the two sectioning techniques, light sheet microscopy performs better (E = 0.0172), with significantly less high-frequency noise compared to the confocal image (E = 0.0491). It is worth noting that the light sheet system outperforms confocal microscopy despite the lower numerical aperture detection objective (0.9 versus 1.42). Not only does the lower numerical aperture reduce the number of photons captured, but it also increases the magnitude of the blurring that needs to be used to calculate the RMSE, meaning that noise contributes more strongly to the RMSE in the light sheet case. We calculated RMSE values for the normalised intensity images using MATLAB.

In contrast to widefield and confocal microscopy stacks, the light sheet images require post-imaging processing, specifically a procedure called deskewing. This is necessary to correct for the angle at which the light sheet intersects the sample surface in our setup (48° with respect to the stage plane) to reconstruct the pictures in a conventional geometry. The deskewing can be performed with an affine transformation where each image slice is computationally shifted (deskewed) to its proper position in the three-dimensional image volume. This procedure was performed using a customized ImageJ macro based on the TranformJ ImageJ plugin[16,9].

3.4 Expansion microscopy highlights the vesicular structure of NP-containing compartments

By combining expansion and light sheet microscopy we could generate high-contrast 3D reconstructions of whole infected cells. In Figure 4A, we show maximum intensity projections at different magnification obtained from a light sheet image z-stack after deskewing. Using the z-stacks acquired combining expansion microscopy and light sheet microscopy we could render 3D models of whole LAIV-infected A549 cells with high contrast, as shown in Figure 4A (fourth row) and Supporting Video 2. The resolution increase brought about by the sample expansion allowed us to demonstrate that the LAIV nucleoprotein localises at or in the membrane of small vesicular structures in the cell cytosol (Figure 4, third row). It is well known that viral ribonucleoprotein complexes (vRNP) of influenza A virus which are formed by nucleoprotein, viral RNA and other viral proteins are transported to sites of virion formation at the plasma membrane by use of recycling endosomes.[17,18] Taking the calculated

expansion factor of 4.2 (Figure 4B) into account, we find that the vesicles possess a diameter of up to ~500 nm (see size distribution in Figure 4C). The smallest vesicle diameter that we could resolve is ~150 nm. In contrast, before expanding the sample we were not able to resolve the vesicular structure of the compartments occupied by the viral nucleoprotein (Figure 1). Interestingly, we find that the larger vesicles preferably occupy a space next to the nucleus where typically the Golgi apparatus is positioned whereas the smaller vesicles are closer to the cell periphery. The space occupied by the larger vesicles is almost devoid of microtubules, and the vesicles do not seem to directly interact with the microtubules. This is interesting and in line with observations for influenza A virus which suggests that the mode of transport for vRNP complexes can be microtubule-independent.[19] Moreover, there was no identifiable DNA compaction inside the nucleus, which is typical of other viruses such as herpes.[20] In the future, we aim to use this technique for studying the interplay between the viral proteins and the cell compartments in order to dissect the whole replication cycle of LAIV.

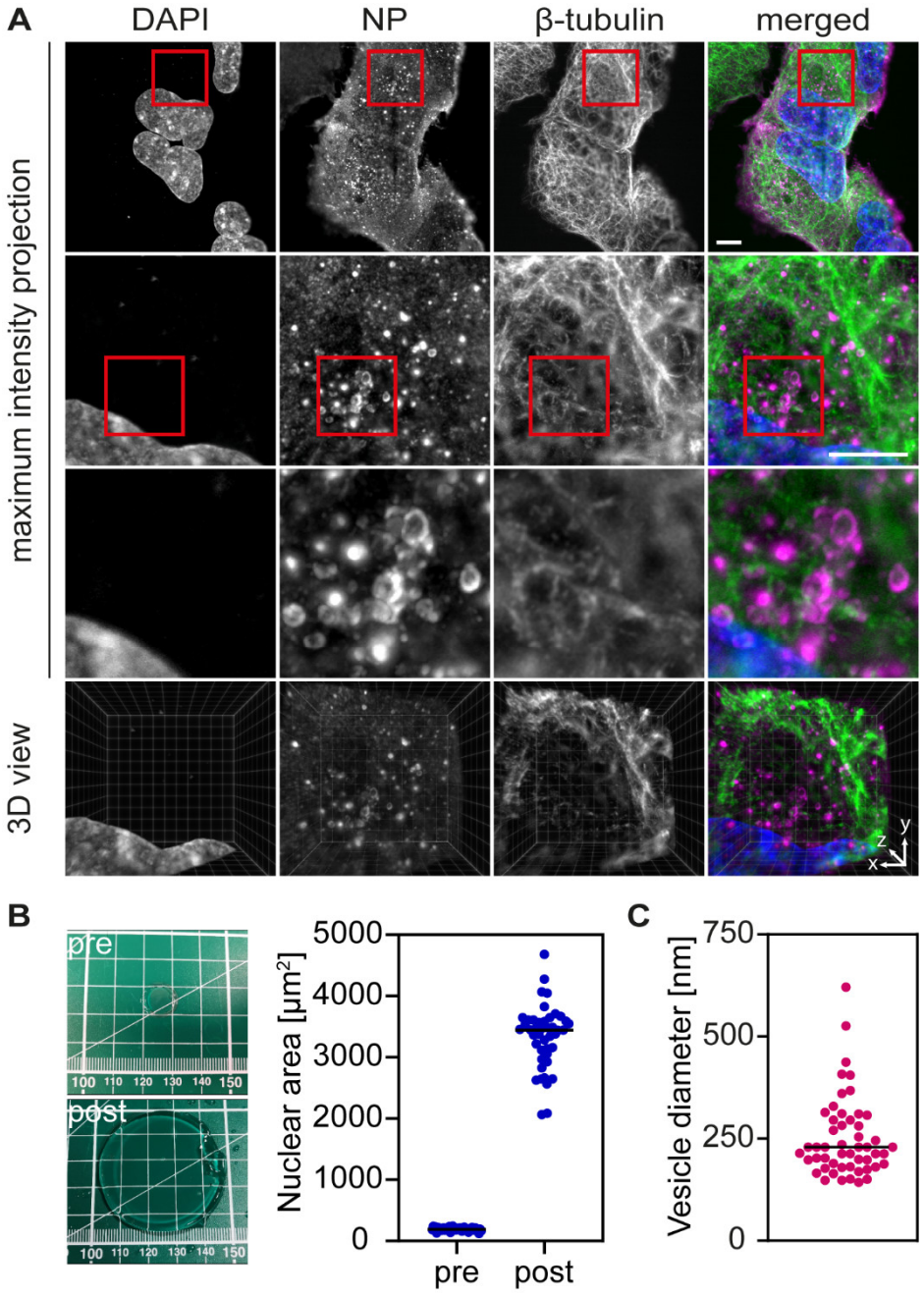

Figure 4: (A) Maximum intensity projections of expanded A549 cells infected with live attenuated influenza vaccine (LAIV). The expansion allows resolving the structure of the viral nucleoprotein NP, which forms vesicular structures in the cytosol before the virus egress. Cells were fixed 9 hours post infection, immunostained, expanded and imaged using a light sheet microscope. Cell nuclei are shown in blue, LAIV nucleoprotein (NP) in magenta and microtubules in green. Scale bar 20 µm. Images in the third row are 20 x 20 μm^2. Fourth row shows a snapshot by the ClearVolume plugin for ImageJ[21] which was used to generate Supplementary Video 2. (B) A linear expansion factor of 4.2 (corresponding to a volumetric expansion factor of 74) was calculated by measuring the gel size before and after expansion (left panel), as well as by measuring the area of 50 cell nuclei before and after expansion (right panel). (C) The expansion factor was used to calculate the size of the NP-containing vesicles.

4. Conclusions

In this work, we imaged LAIV-infected A549 cells using a combination of expansion microscopy and light sheet microscopy, as well as confocal and widefield microscopy. The 3D rendering of whole infected cells was impossible using the data obtained from the confocal microscope, since the acquisition time and photobleaching of this instrument are incompatible with the recording of z-stacks. The widefield microscope did not possess enough sectioning resolution and was characterised by low image contrast, thus, it could not produce cell reconstructions with a sufficient level of detail for our purpose. The light sheet microscope, instead, could scan the whole specimen and delivered 3D renderings of whole infected cells with high contrast. We, therefore, concluded that the combination of light sheet and expansion microscopy was the best in order to image virus-infected cells, as it allows to visualise the interplay between the viral proteins and the cell organelles with high contrast and high resolution in whole cells.

In terms of sample mounting and imaging, the light sheet microscope poses some issues as regards the gel nature of the sample. To this end, we showed a step-by-step video protocol that clarifies how a gelled sample can be imaged using this instrument. In our experience, after getting accustomed to the mounting of the sample, imaging at the light sheet microscope was faster than imaging at either the widefield microscope or the confocal microscope.

By combining light sheet and expansion microscopy, we could visualise details that were not visible in the non-expanded sample, such as the LAIV nucleoprotein in vesicular compartments inside the cell cytoplasm, while simultaneously visualising other cellular structures like the cell nucleus and the cell microtubules. In the future, we aim to use the combination of light sheet and expansion microscopy to map the whole LAIV life cycle at super-resolution and to clarify the relationship between the viral structures and the cellular compartments.

Expansion microscopy is a technique that is not yet widely explored in the field of virology. However, it has enormous potential to study relevant questions not only for LAIV, but viruses and their respective host cell biology in general. The continuous development of new protocols will allow the investigation of distinct events in the viral life cycle like entry, assembly and egress in high resolution since viral proteins, host cell proteins and even viral RNA can potentially be visualised at the same time. Here, we have demonstrated the optimal way to image expanded samples and access the additional information that is gained through the increase in resolution due to physical sample magnification. In general, we think that this combination of techniques is ideal for all the biological applications that require fast, high-contrast and high-resolution imaging in 3D. We hope that this work will help spread the combination of expansion microscopy and light sheet microscopy in biological laboratories worldwide.

Acknowledgements

CFK acknowledges funding from the UK Engineering and Physical Sciences Research Council, EPSRC (grants EP/L015889/1 and EP/H018301/1), the Wellcome Trust (grants 3-3249/Z/16/Z and 089703/Z/09/Z) and the UK Medical Research Council, MRC (grants MR/K015850/1 and MR/K02292X/1), AstraZeneca, and Infinitus (China) Ltd. We thank James Manton for constructing the

light sheet microscope used in this work, as well as providing image processing software. We also thank Francesca van Tartwjik for proofreading the manuscript.

References

1. Chen, F., Tillberg, P. W. & Boyden, E. S. Expansion microscopy. *Science (80-.).* **347,** 543–548 (2015).
2. Wassie, A. T., Zhao, Y. & Boyden, E. S. Expansion microscopy: principles and uses in biological research. *Nature Methods* **16,** 33–41 (2019).
3. Siedentopf, H. & Zsigmondy, R. Uber Sichtbarmachung und Größenbestimmung ultramikoskopischer Teilchen, mit besonderer Anwendung auf Goldrubingläser. *Ann. Phys.* **315,** 1–39 (1902).
4. VOIE, A. H., BURNS, D. H. & SPELMAN, F. A. Orthogonal-plane fluorescence optical sectioning: Three-dimensional imaging of macroscopic biological specimens. *J. Microsc.* **170,** 229–236 (1993).
5. Huisken, J., Swoger, J., Del Bene, F., Wittbrodt, J. & Stelzer, E. H. K. Optical Sectioning Deep Inside Live Embryos by Selective Plane Illumination Microscopy. *Science (80-.).* **305,** 1007 LP-1009 (2004).
6. Chhetri, R. K. *et al.* Whole-animal functional and developmental imaging with isotropic spatial resolution. *Nat. Methods* **12,** 1171–1178 (2015).
7. Arrenberg, A. B., Stainier, D. Y. R., Baier, H. & Huisken, J. Optogenetic Control of Cardiac Function. *Science (80-.).* **330,** 971 LP-974 (2010).
8. Mickoleit, M. *et al.* High-resolution reconstruction of the beating zebrafish heart. *Nat. Methods* **11,** 919–922 (2014).
9. Meijering, E. H. W., Niessen, W. J. & Viergever, M. A. Quantitative evaluation of convolution-based methods for medical image interpolation. *Med. Image Anal.* **5,** 111–126 (2001).
10. Chan, W., Zhou, H., Kemble, G. & Jin, H. The cold adapted and temperature sensitive influenza A/Ann Arbor/6/60 virus, the master donor virus for live attenuated influenza vaccines, has multiple defects in replication at the restrictive temperature. *Virology* **380,** 304–311 (2008).
11. He, W. *et al.* Molecular Basis of Live-Attenuated Influenza Virus. *PLoS One* **8,** e60413 (2013).
12. Chozinski, T. J. *et al.* Expansion microscopy with conventional antibodies and fluorescent proteins. *Nat. Methods* **13,** 485–488 (2016).
13. Wu, Y. *et al.* Inverted selective plane illumination microscopy (iSPIM) enables coupled cell identity lineaging and neurodevelopmental imaging in Caenorhabditis elegans *Proc. Natl. Acad. Sci.* **108,** 17708 LP-17713 (2011).
14. Dou, D., Revol, R., Östbye, H., Wang, H. & Daniels, R. Influenza A virus cell entry, replication, virion assembly and movement. *Frontiers in Immunology* **9,** (2018).
15. Gao, R., Asano, S. M. & Boyden, E. S. Q&A: Expansion microscopy. *BMC Biol.* **15,** 50 (2017).
16. TransformJ. Available at: https://imagescience.org/meijering/software/transformj/.
17. de Castro Martin, I. F. *et al.* Influenza virus genome reaches the plasma membrane via a modified endoplasmic reticulum and Rab11-dependent vesicles. *Nat. Commun.* **8,** 1396 (2017).
18. Eisfeld, A. J., Kawakami, E., Watanabe, T., Neumann, G. & Kawaoka, Y. RAB11A Is Essential for Transport of the Influenza Virus Genome to the Plasma Membrane. *J. Virol.* **85,** 6117 LP-6126 (2011).
19. Bhagwat, A. R. *et al.* Quantitative live cell imaging reveals influenza virus manipulation of Rab11A transport through reduced dynein association. *Nat. Commun.* **11,** 23 (2020).
20. Monier, K., Armas, J. C. G., Etteldorf, S., Ghazal, P. & Sullivan, K. F. Annexation of the interchromosomal space during viral infection. *Nat. Cell Biol.* **2,** 661–665 (2000).
21. Royer, L. A. *et al.* ClearVolume: open-source live 3D visualization for light-sheet microscopy. *Nature methods* **12,** 480–481 (2015).

SUPPLEMENTARY INFORMATION

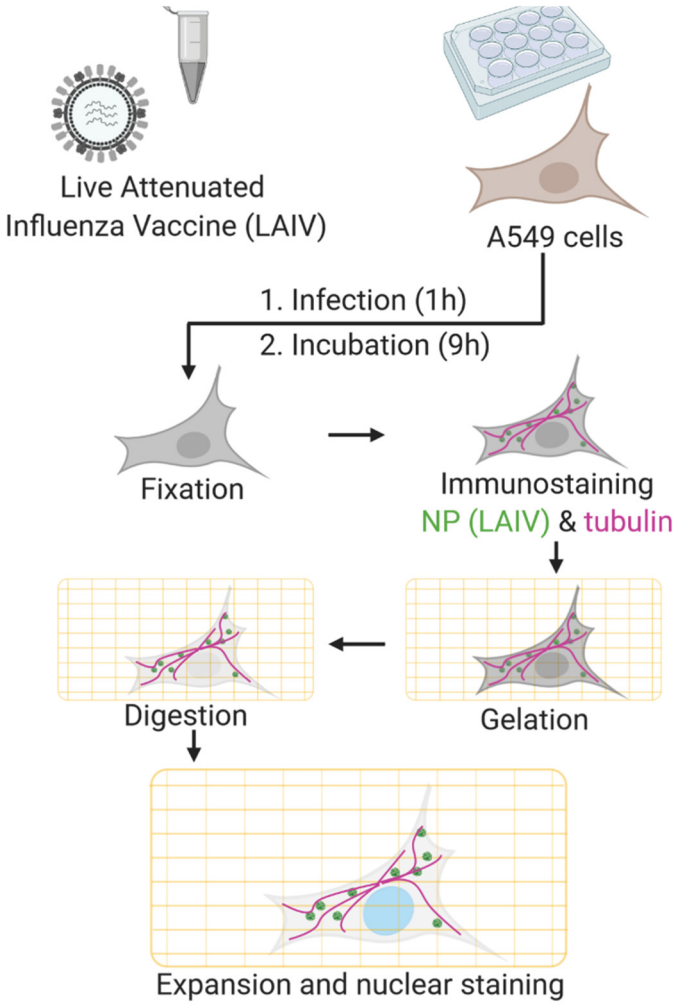

Supporting Figure 1: Schematic rendering of the infection with Live Attenuated Influenza Vaccine, immunostaining and expansion of A549 cells. Image created using BioRender.

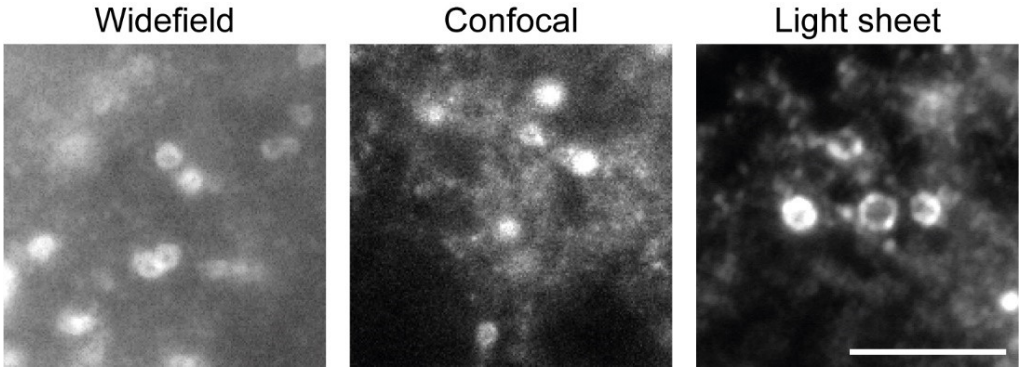

Supporting Figure 2:Details of vesicular structures in the cytosol of expanded A549 cells infected with Live Attenuated Influenza Vaccine (LAIV nucleoprotein channel). The same sample was imaged using either a widefield, confocal or light sheet microscope. Scale bar 20 µm.

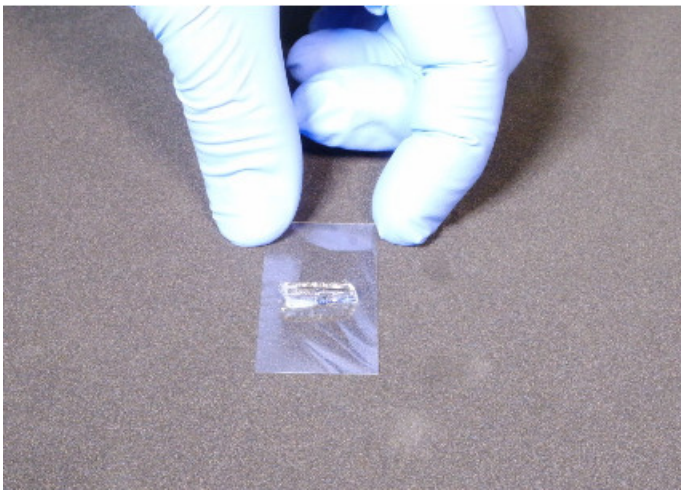

Supporting Video 1: This viedo shows a detailed step-by-step procedure for the mounting of a sample expanded by means of expansion microscopy using a light sheet microscope.

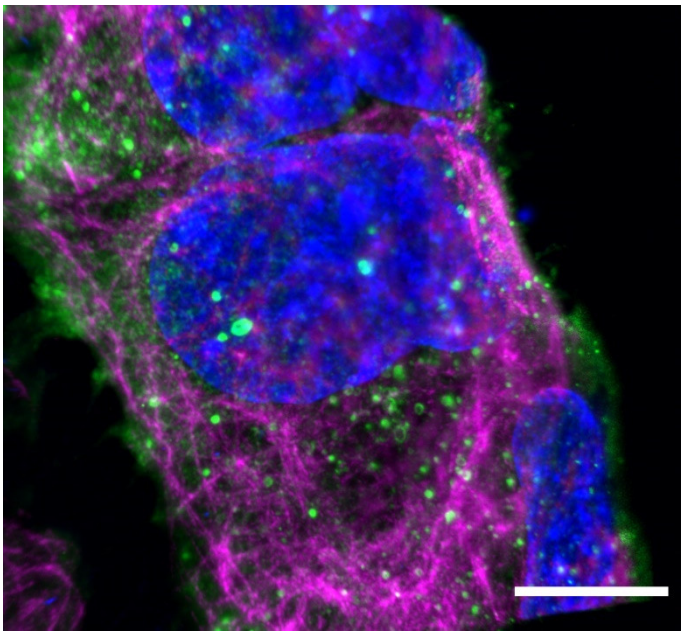

Supporting Video 2: 3D rotation of an expanded sample (A549 cells infected with Live Attenuated Influenza Vaccine) imaged at a light sheet microscope. Blue shows DAPI staining of the cell nucleus, green the LAIV nucleoprotein (NP) and magenta the cell microtubules. Scale bar 20 µm.